APJAI
Asian Pacific Journal of
Allergy and Immunology

ORIGINAL ARTICLE

Chimeric peptides targeting the receptor-binding domain of SARS-CoV-2 variants inhibit ACE2 interaction

Pisit Ubonsri, Jiraporn Panmanee, Ittipat Meewan, Promsin Masrinoul, Jukrapun Komaikul, Surapon Piboonpocanun

Abstract

Background: The receptor-binding domain (RBD) of the SARS-CoV-2 spike (S) protein is pivotal in facilitating viral entry and serves as a major target for vaccine development and therapeutics. Despite undergoing mutations aimed at evading host immunity, certain regions within the RBD remain conserved.

Objective: This study aimed to identify peptides capable of interacting with these conserved regions of the RBD across various variants and assess their neutralization potential.

Methods: The PhD-12 phage display library underwent screening to identify phages binding to the RBD. Selected phage clones were examined for binding to the RBD of multiple variants, including 2019-nCoV, Delta (B.1.617.2), Omicron (B.1.1.529), and XBB. Peptides, expressed as chimeric constructs, were tested for their binding to the RBD, the Omicron trimeric S, inactivated SARS-CoV-2 virus, and neutralizing activity. The binding sites were analyzed using Molecular Docking.

Results: Two selected phage clones displayed peptides binding to the RBD of multiple variants. Chimeric Thioredoxin-peptides (Trx-RB9 and Trx-RB10) exhibited binding to both inactivated SARS-CoV-2 and the Omicron trimeric S, with half-maximum effective concentrations (EC_{50}) values of 111.9 and 360.2 nM, respectively. Molecular docking revealed distinct binding sites within the RBD of the Omicron trimeric S for both Trx-RB9 and Trx-RB10. A mixture of Trx-RB9 and Trx-RB10 inhibited 78% of the binding of recombinant human ACE2 to the Omicron trimeric S.

Conclusions: The chimeric Trx-RB9 and Trx-RB10 peptides bind to the RBD of SARS-CoV-2 variants and inhibit the binding of ACE2 to the RBD of the Omicron trimeric S.

Key words: SARS-CoV-2, phage display, peptides, receptor-binding domain (RBD), angiotensin-converting enzyme 2 (ACE2), respiratory disease

Citation:
Ubonsri, P., Panmanee, J., Meewan, I., Masrinoul, P., Komaikul, J., Piboonpocanun, S. (0000). Chimeric peptides targeting the receptor-binding domain of SARS-CoV-2 variants inhibit ACE2 interaction. *Asian Pac J Allergy Immunol*, 00(0), 000-000. https://doi.org/10.12932/ap-030424-1833

Affiliation:
Institute of Molecular Biosciences, Mahidol University, Salaya, Nakhon Pathom, Thailand

Corresponding author:
Surapon Piboonpocanun
Institute of Molecular Biosciences, Mahidol University, Salaya, Nakhon Pathom, Thailand
E-mail: surapon.pib@mahidol.edu

Introduction

The emergence of severe acute respiratory syndrome coronavirus 2 (SARS-CoV-2), the causative agent of COVID-19, in late 2019 underscored a significant global public health concern. Individuals infected with underlying medical conditions are predisposed to developing severe symptoms.[1-3] SARS-CoV-2, a novel coronavirus within the Coronaviridae family, is characterized by its single-stranded, positive-sense RNA genome (+ssRNA). The spike (S) protein, located on the viral envelope, comprises two distinct functional subunits: S1 and S2.[4-6] The receptor-binding domain (RBD) of the S1 subunit, binding to the host's angiotensin-converting enzyme 2 (ACE2) receptor, is a crucial initial interaction that facilitates the complex process of viral entry and replication within the host.[7-9]

From these findings, the RBD appears to be a crucial target for the development of antibodies for neutralization and detection.[10,11] However, SARS-CoV-2 has the remarkable ability to adapt and undergo genetic changes in the S protein, resulting in the emergence of multiple variants, including Alpha (B.1.1.7), Delta (B.1.617.2), and Omicron (B.1.1.529).[7,12,13] These variants affect vaccine efficacy and the efficiency of neutralizing antibodies and the detection of antibodies. Within a defined timeframe, the expedited development of peptides with both neutralizing and detecting capabilities may be desirable.[14-19] Phage display is a robust technique for identifying short peptides, typically 7-12 amino acids long. Mimicking those on the Fab regions of antibodies, these short peptides interact with specific targets with high affinity. With a library of over a billion unique phages displaying diverse short peptides, this method enables extensive screening and analysis for both neutralizing and detecting viruses more efficiently.[20,21] In the context of the ongoing COVID-19 pandemic, identifying and characterizing peptides that bind specifically to the RBD of the S proteins of SARS-CoV-2 could serve as invaluable tools for viral detection and neutralization.

This study aimed to identify peptides that interact with the RBD using a phage display library. Subsequently, selected displayed peptides, expressed as chimeric constructs, underwent evaluation for binding affinity to the RBD of various SARS-CoV-2 variants, including the Omicron trimeric S. Additionally, their ability to neutralize the binding of ACE2 to the Omicron trimeric S was assessed.

Methods

Phage display selection against the RBD of SARS-CoV-2

An amount of 18.87 μM of the recombinant RBD of SARS-CoV-2 with a 6xHis tag (Sino Biological, China) was coupled with Ni^{2+} magnetic beads (Sigma, USA). Subsequently, the beads were incubated in a TBS-0.1% Tween-20 (T) and 1% bovine serum albumin (BSA) solution (50 mM Tris-HCl, pH 7.5) before being used in biopanning, as described in the manufacturer's manual and the Supplementary Methods.

Phage ELISA

The binding of the eluted phages to the RBD of SARS-CoV-2 was determined. An amount of 188.68 nM of the RBD in PBS-1% BSA was coated in each well of a 96-well Maxisorp plate (Nunc, USA) before being incubated with 0.5×10^8 pfu/mL of amplified phages. Bound phages were detected using HRP-labeled mouse IgG anti-M13 phage (Abcam, UK) as described in the Supplementary Methods.

Expression and purification of chimeric peptides

The phage-derived 12-amino-acid peptides were expressed as chimeric bacterial Thioredoxin (Trx) fused proteins (Trx-RB) using the plasmid pET32b (GenScript, USA). All chimeric fused proteins, including Trx-RB and a chimeric Trx fused with an unrelated target peptide (Trx-UTP), were expressed and prepared as described in the Supplementary Methods and used in all experiments.

Direct binding of Chimeric Trx-peptides

The avidin tags of Trx peptides (Trx-RB) and the Trx-unrelated-target-peptide (Trx-UTP) were biotinylated using a biotinylation kit (Abcam, UK). The binding of biotinylated Trx-RB and Trx-UTP to the recombinant RBD (aa328-525) of the S1 of variants, including SARS-CoV-2, Delta, Omicron, and XBB (Sino biological, China), was performed as described in the Supplementary Methods.

EC_{50} determination assay using the SARS-CoV-2 (B.1.1.529) trimeric S

To determine the half-maximal effective concentration (EC_{50}), a serial dilution of 0.1 to 600 nM biotinylated Trx-RB9 and Trx-RB10 was prepared. The binding of these Trx-peptides to 7.14 nM of recombinant trimeric S (S1 + S2) of SARS-CoV-2 (B.1.1.529, Omicron) (Omicron trimeric S) (Sino Biological, China) was performed as described in the Supplementary Methods. A serial dilution of 0.01 to 100 nM recombinant human ACE2 with a human FC tag (ACE2-FC) (Sino Biological, China) was included as the control.

Analysis of binding sites of chimeric Trx-RB on the RBD of the SARS-CoV-2 (B.1.1.529) trimeric S

The binding sites of Trx-RB9 and Trx-RB10 on the RBD of the Omicron trimeric S were determined using competitive ELISA and Western blot. Both protocols are described in the Supplementary Methods. In the competitive ELISA, 7.14 nM of Omicron trimeric S in PBS, 100 nM biotinylated-Trx-RB10, and various dilutions of Trx-RB9 (0, 62.5, 125, 250, 500 nM) were used. For the Western blot, 59.52 nM of Omicron trimeric S was loaded per lane and transferred onto a nitrocellulose membrane. A mixture of 5 nM ACE2-Fc and 500 nM Trx-RB9 and/or Trx-RB10 was also used in these analyses.

Direct ELISA of the chimeric Trx-RB binding the inactivated SARS-CoV-2

SARS-CoV-2 (2019-nCoV; MUMT64019039) propagation and inactivation protocols are described in the Supplementary Methods. For ELISA, a diluted 10^2-10^7 pfu/mL of inactivated SARS-CoV-2 in PBS, along with 600 nM of biotinylated-Trx-RB9, Trx-RB10, and Trx-UTP, were used. The detailed protocol is described in the Supplementary Methods.

Molecular docking for chimeric Trx-peptides interacting with the Omicron spike

The predicted 3D structure of chimeric Trx-peptides was obtained from the ColabFold web server.[22] The protein structures of Omicron trimeric spike (PDB: 7WVN and PDB: 7WPD), the RBD of Omicron spike (PDB: 7WPB), and human ACE2 (PDB: 6JWH) were obtained from the Protein Data Bank (PDB) web server (https://www.rcsb.org). Molecular docking of chimeric peptides or ACE2 with the spike protein was performed using the binding site-specific flexible docking approach on the HADDOCK web server.[23]

Structure comparison and visualization of Omicron trimeric spike and the RBD of Omicron spike were performed using ChimeraX (Matchmaker tools). Alignment of the secondary structures of proteins was performed by the Needleman-Wunsch algorithm.

Data and statistical analysis

The data analysis was conducted using Prism9 (GraphPad, USA). Mean differences between the peptides and the negative control were assessed using unpaired Student's t-tests. *P*-values were calculated using a two-tailed ANOVA test with a 95% confidence level.

Results

Biopanning of phage display binding the RBD of the SARS-CoV-2

The PhD-12 phage display library underwent screening or biopanning to identify phages that bind to the RBD of SARS-CoV-2 (**Figure 1a**). The number of phages binding to the RBD from the first, second, and third rounds of biopanning, was 2.4×10^5, 8×10^5, and 6.5×10^7 viral phages, respectively. Additionally, OD_{450nm} values of phages bound the RBD in the first, second, and third rounds, were 0.445, 0.627, and 0.957, respectively (**Figure 1b**). From 120 selected phages from the three rounds of biopanning, 5 individual clones (RB5, RB9, RB10, RB54, and RB56) were identified.

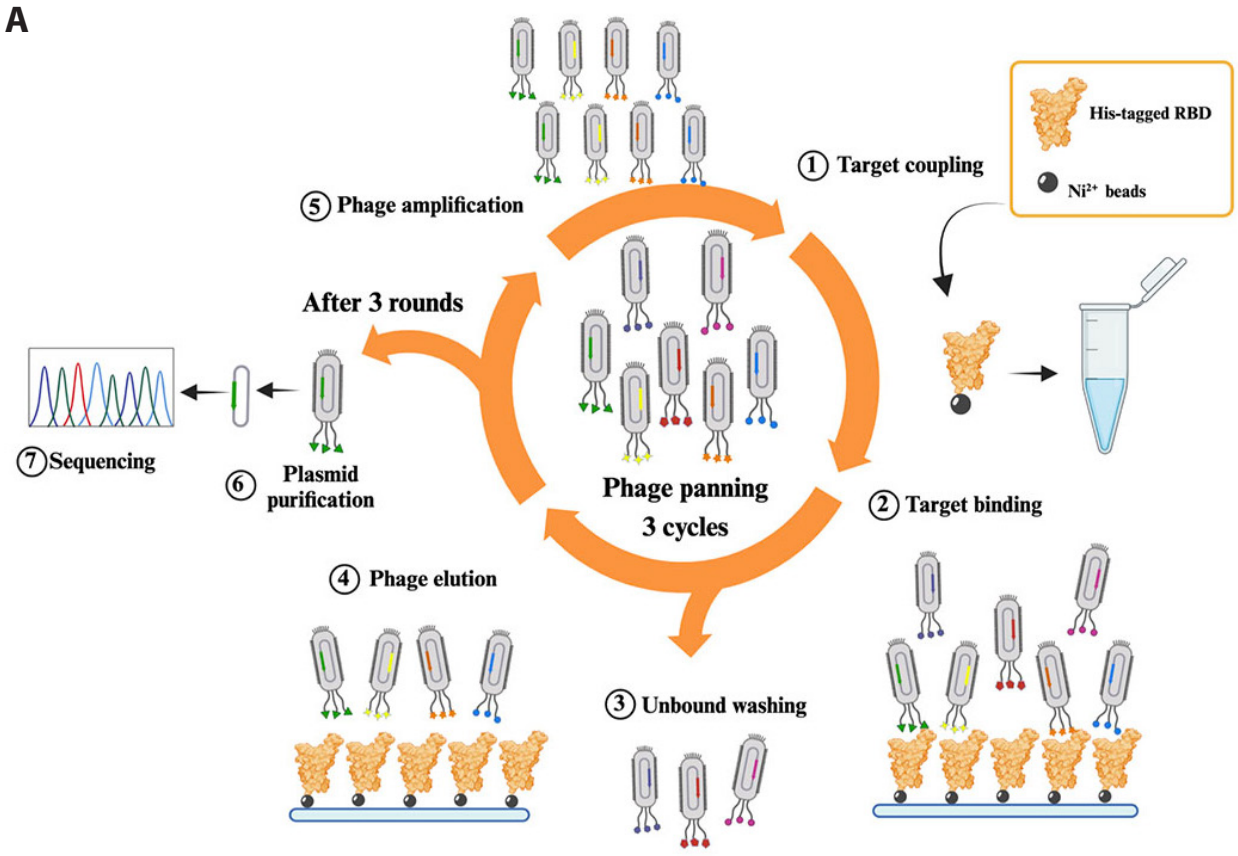

Figure 1. Biopanning of Phages Binding to the RBD and Phage ELISA. (a) Schematic illustrating the methodology employed for the phage display biopanning. (b) The RBD binding results of three rounds of biopanning. (c) The RBD binding results of 5 selected phage clones: RB5, RB9, RB10, RB54, and RB56.

Note: a non-specific control, phages binding to BSA.

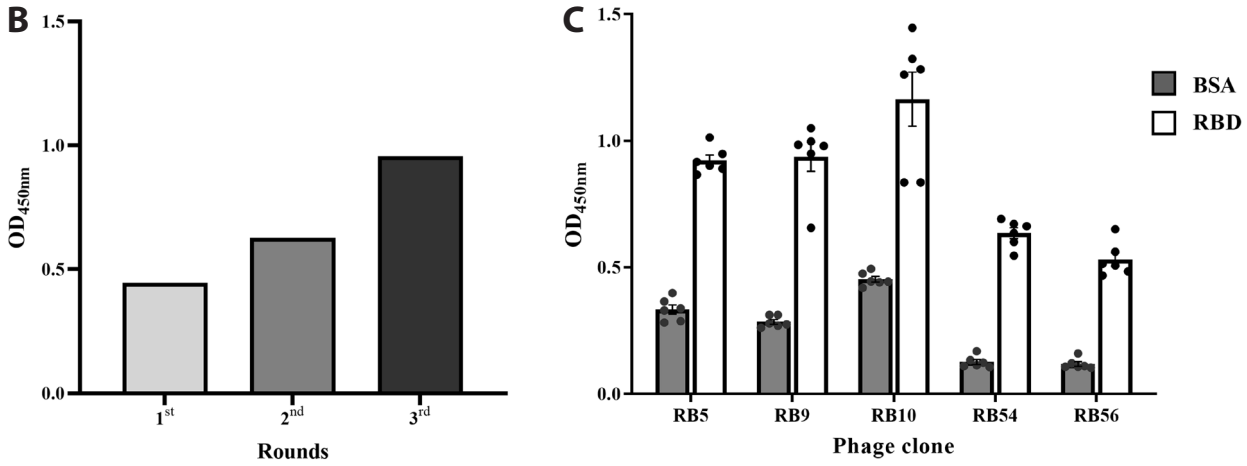

Figure 1. (Continued)

Table 1. Characteristic of chimeric Trx-peptides.

Peptide	Sequence	Molecular weight	*pI*	Solubility of chimeric Trx-peptide	*Water Solubility of peptides	UTP scan	Reported peptides
RB5	Trx-avidin-GTYYLYGVGSEA	20953.41	5.14	0.780	Poor	NM	NM
RB9	Trx-avidin-ESYSAKHRIMLT	21109.71	5.47	0.800	Good	NM	NM
RB10	Trx-avidin-ATMRGDQSVRIF	21054.63	5.37	0.793	Good	NM	NM
RB54	Trx-avidin-HYHLHSHGMVQR	21175.73	5.71	0.792	Poor	NM	NM
RB56	Trx-avidin-HLRHVATDHHAP	21064.57	5.60	0.818	Good	NM	NM
UTP	Trx-avidin-FAIPLVVPFYSH	21063.71	5.34	0.759	Poor	NM	NM

Note: *Water Solubility analyzed by PepCalc (www.pepcalc.com); *pI*, isoelectric point; UTP, unrelated target peptides; NM, no match

These clones exhibited binding the RBD with OD_{450nm} values ranging from 0.58 to 0.71 after subtracted background signals and were selected for characterization of binding activities. DNA sequence of the selected clones was obtained (**Figure 1c**). Their deduced peptide sequences had no identity or similarity to either unrelated target peptides (UTP) or reported peptides from the SAROTUP and UniProt web servers (**Table 1**).

Characterization of chimeric Thioredoxin-RBD binding peptides

Chimeric Thioredoxin fused RBD binding peptides (Trx-RB) derived from RB5, RB9, RB10, RB54, and RB56 were characterized (**Table 1**). All purified chimeric Trx-RB peptides mobilized between the 20-25 kDa markers in SDS-PAGE gels (**Figure S1**). Furthermore, immunoblotting using anti-His mAb confirmed their identity. Predicted structural features of the five chimeric Trx-RB peptides generated by ColabFold exhibited an unstructured conformation of the fused RB peptides, with a model confidence score of < 70 pDLLT (**Figure S2**). In contrast, the Trx component retained its structural integrity, as evidenced by a model confidence score exceeding 90 pDLLT (**Figure S2**).

Binding characteristic of chimeric Trx-RB peptides

The ELISA results demonstrated that four chimeric Trx-RB peptides (RB5, RB9, RB10, RB54) binding to the RBD of the SARS-CoV-2 with OD_{450nm} values exceeding 0.75, while Trx-RB56 and Trx-UTP showed a similar 0.5 OD_{450nm} value (**Figure 2a**). Further binding to the recombinant SARS-CoV-2 RBD variants, including Delta, Omicron, and XBB, revealed that only Trx-RB9 and Trx-RB10 interacted with all three variants, with varying affinities (**Figure 2b-d**). Specifically, Trx-RB9 bound the RBD of the Delta, Omicron, and XBB variants, with OD_{450nm} values of 0.50, 1.30, and 0.43, respectively (**Figure 2b-d**). Moreover, Trx-RB10 bound the RBD of the Delta, Omicron, and XBB variants, with OD_{450nm} values of 0.58, 0.62, and 0.36, respectively (**Figure 2b-d**). Analysis of the binding of both Trx-RB9 and Trx-RB10 to the Omicron trimeric S showed Trx-RB9 bound with 2 OD_{450nm} value, whereas Trx-RB10 bound with 1.5 OD_{450nm} value (**Figure 2e**). Determination of the half-maximal effective concentration (EC_{50}) of recombinant ACE2 and the chimeric Trx-RB peptides yielded EC_{50} values of 111.9 nM for Trx-RB9 and 360.2 nM for Trx-RB10 bound to the Omicron trimeric S. In comparison, the EC_{50} value for recombinant ACE2 was 1.64 nM (**Figure 3a-c**). Additionally, both Trx-RB9 and Trx-RB10 were directly bound inactivated SARS-CoV-2 at various viral concentrations ranging from 10^5 to 10^7 pfu/mL (**Figure 3d**).

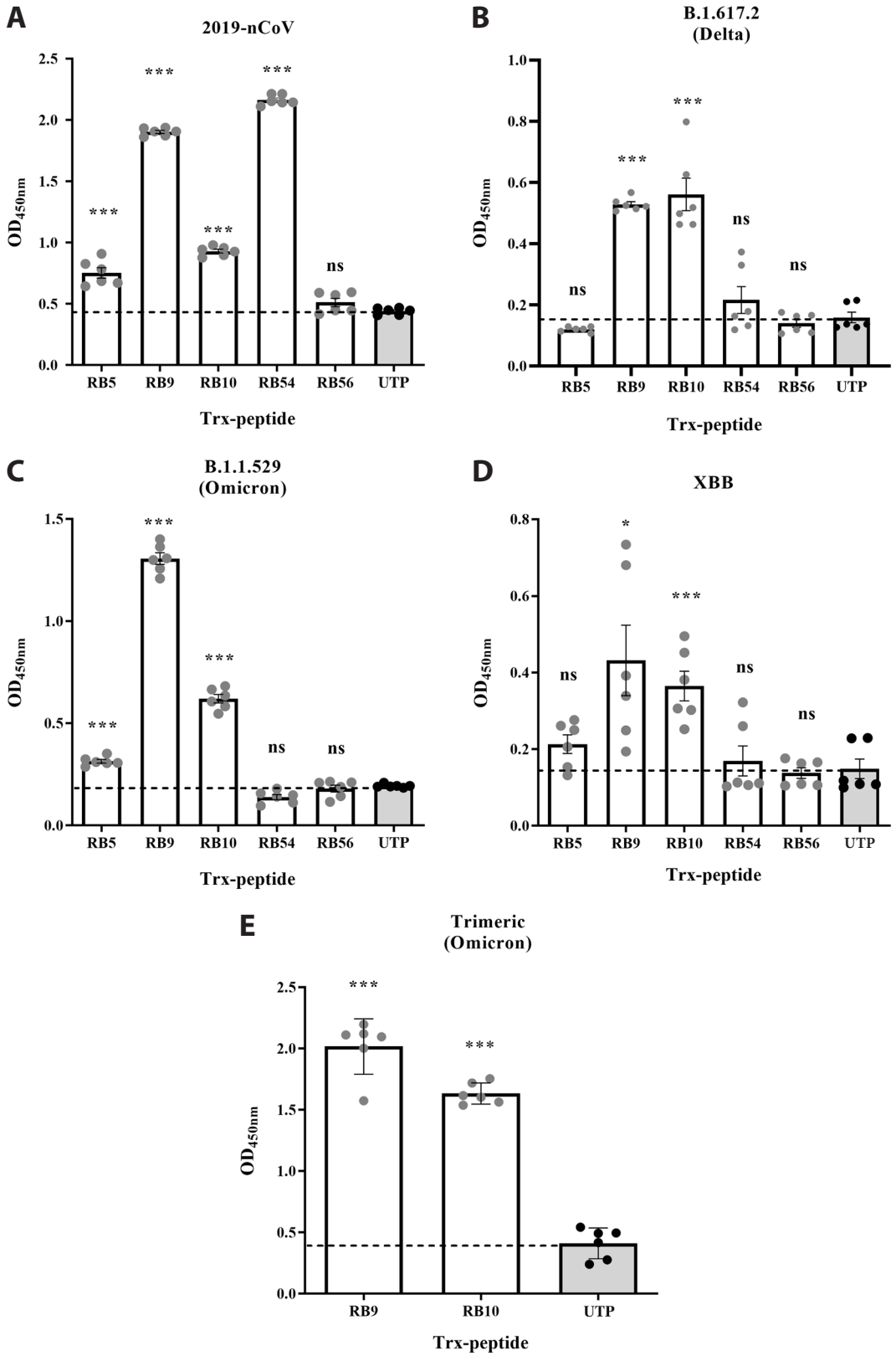

Figure 2. Determining the Binding of Chimeric Peptides to the RBD of SARS-CoV-2 Variants and the Omicron Trimeric S. (a-d) Indirect ELISA of five chimeric peptides (Trx-RB) binding to the RBD of (a) SARS-CoV-2, (b) Delta, (c) Omicron, and (d) XBB. (e) Indirect ELISA of Trx-RB9 and Trx-RB10 binding to the Omicron Trimeric S. Note: Chimeric unrelated target peptide (Trx-UTP) was used as negative control. Data are represented as the mean average ± standard error from three independent experiments. All experiments were performed with at least three independent replicates. *P*-value: **P* < 0.05; **P* < 0.01; ****P* < 0.001; ns, No significant difference vs. Trx-UTP).

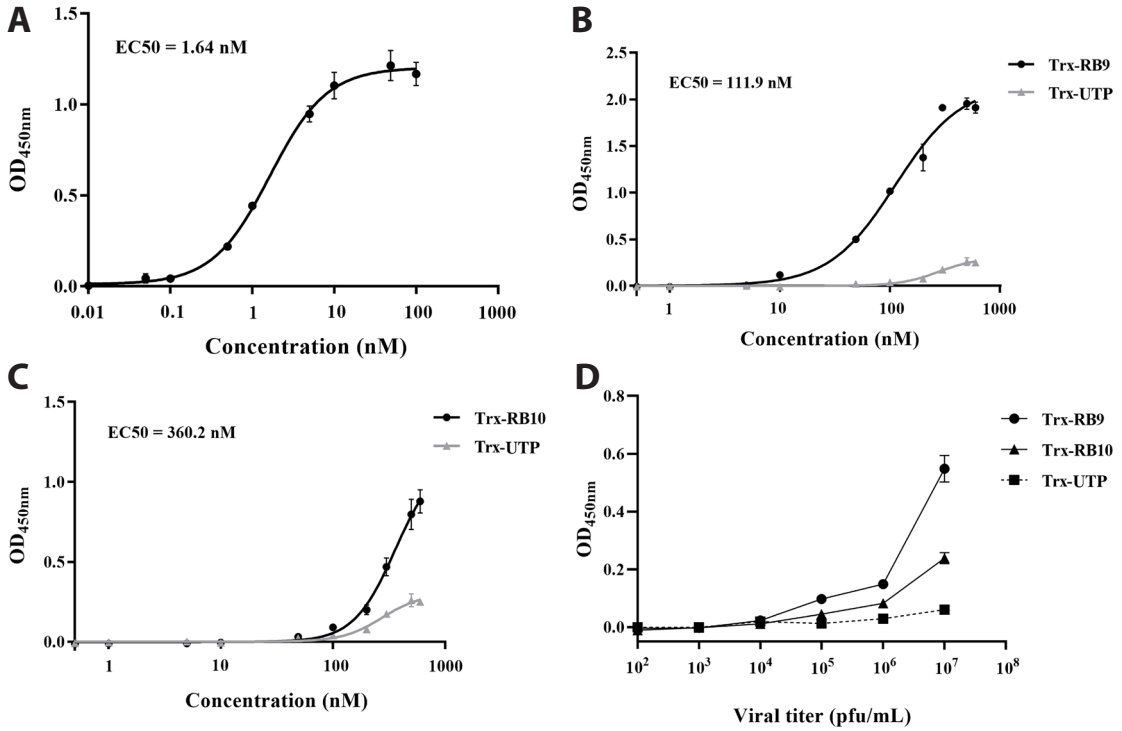

Figure 3. Analysis of Chimeric Trx-RB9 and Trx-RB10 Binding to the Omicron Trimeric S and Inactivated SARS-CoV-2. The binding of (a) ACE2, (b) Trx-RB9, and (c) Trx-RB10 to the Omicron trimeric S. (d) Binding of the biotinylated Trx-RB9, the biotinylated Trx-10, and the biotinylated Trx-UTP to coated inactivated-SARS-CoV-2 (MUMT64019039) at viral titer of 10^2-10^7 pfu/mL.

Mapping binding sites of Chimeric Trx-RB peptides on Omicron trimeric S

The Western blot analysis of binding sites on the RBD of the Omicron trimeric S for Trx-RB9 and Trx-RB10 was conducted. A combination of 250 nM of both Trx-RB9 and Trx-RB10 inhibited 75% of 5 nM recombinant ACE2 binding to the RBD of the Omicron trimeric S (**Figure 4a, b**). However, when incubated individually, neither Trx-RB9 nor Trx-RB10 inhibited the binding of recombinant ACE2 to the RBD of the Omicron trimeric S (**Figure 4b**). To investigate the potential overlap of binding sites for both Trx-RB9 and Trx-RB10, Trx-RB9 was incubated with a mixture of Omicron trimeric S preincubated with biotinylated-chimeric Trx-RB10 (Omicron-RB10). The findings showed that Trx-RB9 marginally reduced the interaction of Omicron-RB10 from 0.359 OD_{450nm} (3.5%) at 62.5 nM to 0.340 OD_{450nm} (8.6%) at 500 nM, compared to the control without Trx-RB10, which yielded 0.372 OD_{450nm} value (**Figure 4c**).

Molecular docking of Chimeric Trx-RB peptides and Omicron trimeric S

The molecular docking analysis demonstrated that Trx-RB9 and Trx-RB10 bound to distinct sites on the RBD of the Omicron trimeric S (**Figure 5a**). Trx-RB9 formed hydrogen bonds with four amino acids on the RBD: GLU1-ILE472, SER4-GLU471, LYS6-ASN460, and THR12-ARG355 (**Figure 5b, c**). Trx-RB10 formed hydrogen bonds with three amino acids on the RBD: ARG4-LEU492,

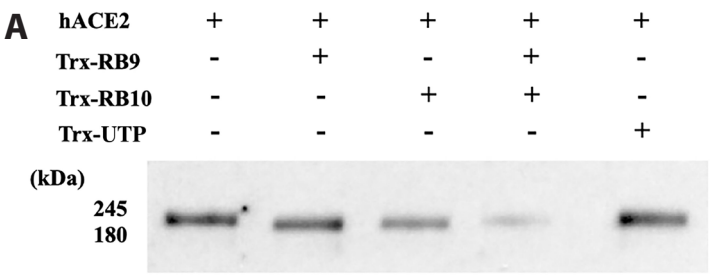

Figure 4. Analysis of Chimeric Peptides Binding Site on the RBD by Western Blot and Inhibition ELISA. (a) Western blot analysis of 500 nM Trx-RB9 and 500 nM Trx-RB10 inhibiting 5 nM ACE2 binding to the Omicron trimeric S. (b) The mean percentage binding of ACE2 to the Omicron trimeric S. Data points represent the mean ± SE of three different experiments. All experiments were performed with three independent replicates. (c) Inhibition ELISA results of chimeric Trx-RB9 inhibiting biotinylated chimeric Trx-RB10 binding to the Omicron trimeric S.

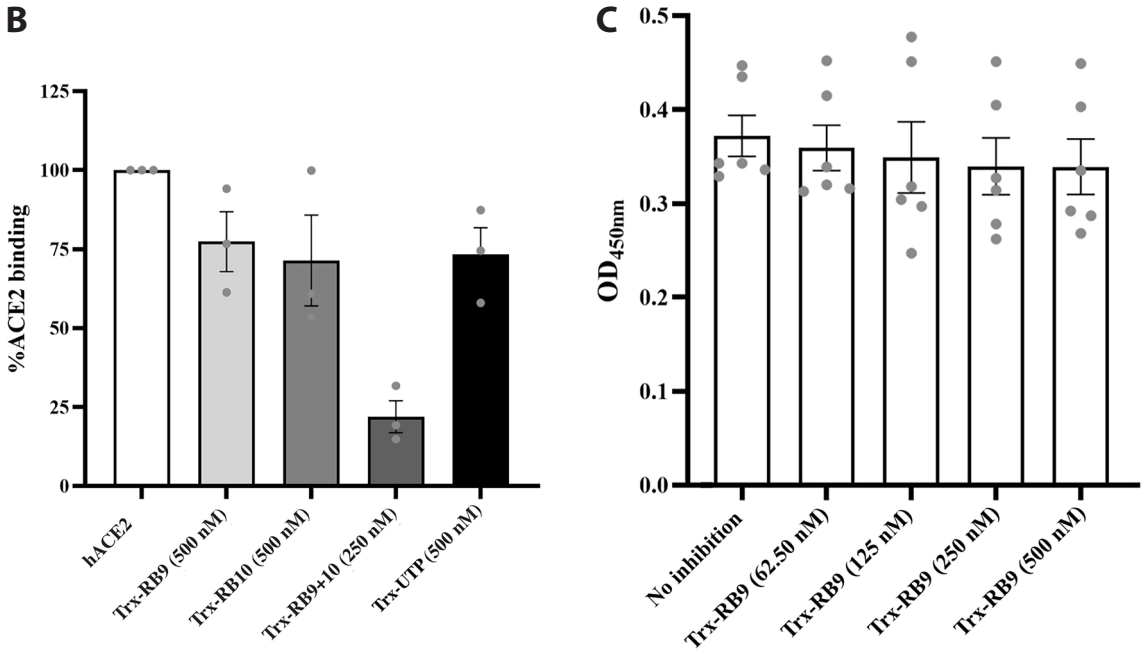

Figure 4. (Continued)

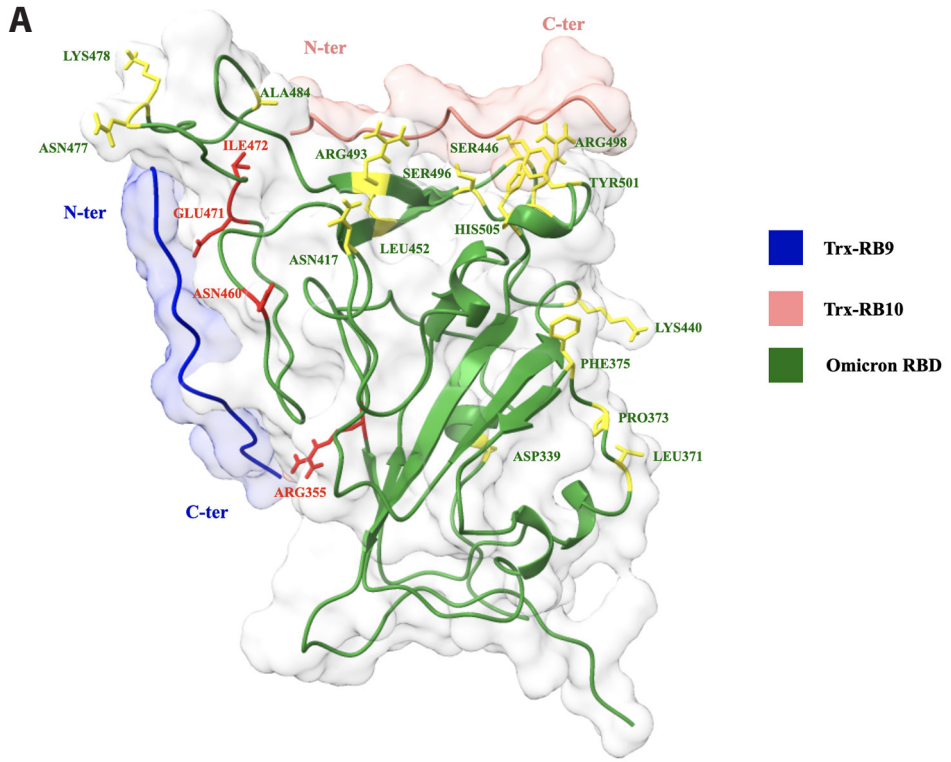

Figure 5. Analysis of Chimeric Peptides' Binding Sites on the RBD by Molecular Docking. (a) Molecular docking using ChimeraX illustrates chimeric Trx-RB9 (blue) and Trx-RB10 (pink) binding to the RBD of the Omicron trimeric S (PDB:7WPD) (green). Note: Mutated amino acids of the RBD are shown in yellow and red; N-ter represents the N-terminus, and C-ter represents the C-terminus. (b) The alignment of amino acid sequences from the RBD of SARS-CoV-2 variants: Delta (B.1.617.2) and Omicron (B.1.1.529). Note: Red letters indicate mutated amino acids; green highlights indicate amino acids that interact with ACE2; * indicates amino acids that interact with Trx-9; ^ indicates amino acids that interact with Trx-RB10. (c) Molecular docking using HADDOCK predicted amino acids of chimeric Trx-RB9 that interact with those on the RBD of the Omicron trimeric S. (d) Molecular docking using HADDOCK predicted amino acids of chimeric Trx-RB10 that interact with those on the RBD of the Omicron trimeric S.

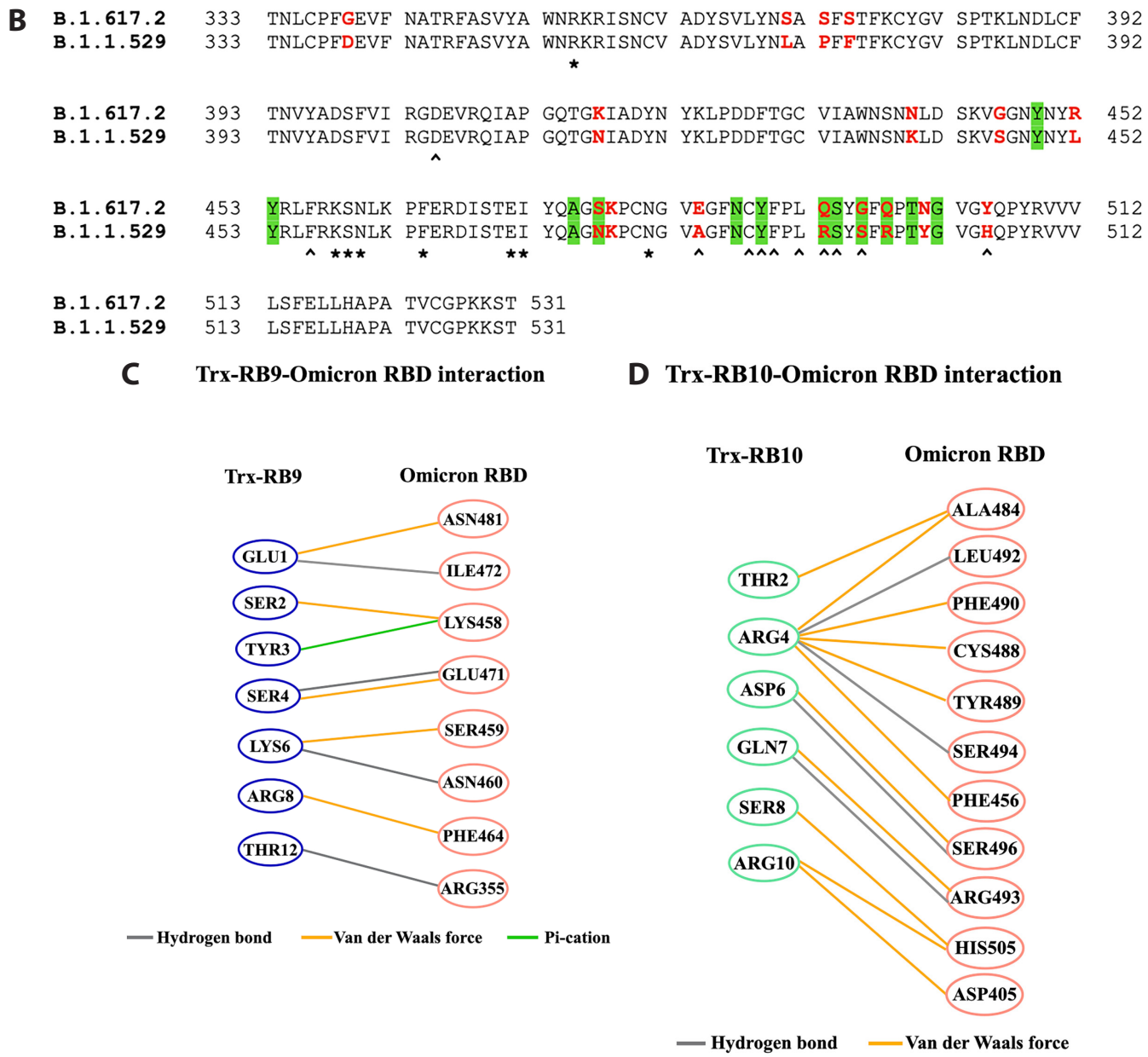

Figure 5. (Continued)

ARG4-SER494, ASP6-SER496, and GLN7-ARG493 (**Figure 5b, d**). The binding site-specific docking score, calculated using HADDOCK, for the binding of Trx-RB9 and Trx-RB10 to the Omicron models was -97.6 ± 19.4 kcal/mol, with a Z score of -0.8 (**Table S1**). A total of 36 structures were generated, forming four clusters or predicted distinct groups, with a Root Mean Square Deviation (RMSD) of the average distance between atoms in the models at 25.3 ± 0.5 angstrom (Å) (**Table S1**). Additionally, the interaction energy between the molecules revealed favorable interactions, with Van der Waals energy (-76.4 ± 13.9 kcal/mol), Electrostatic energy (-297.0 ± 38.5 kcal/mol), and Desolvation (-3.3 ± 2.7 kcal/mol) (**Table S1**). The Buried Surface Area (BSA) value was notably high, measuring 2420.8 ± 192.4 Å^2 (**Table S1**).

To compare Trx-RB binding region with that of human ACE2, the HADDOCK molecular docking analysis between human ACE2 (PDB: 8JWH) and the RBD of the Omicron trimeric spike was also carried out as well as structure of hACE2 interacting RBD was generated by ChimeraX (**Table S2**, **Figure S5**). The HADDOCK score for the model was -97.0 ± 1.7 kcal/mol, with a Z score of -2.0 (**Table S2**). Thirteen clusters or predicted distinct groups were formed with a total of generated 98 structures The models had a Root Mean Square Deviation (RMSD) of the average distance between atoms in the models at 3.3 ± 0.4 Å. The interaction energy between the interacted molecules, Van der Waals energy (-53.5 ± 6.6 kcal/mol), Electrostatic energy (-383.0 ± 13.9 kcal/mol), and Desolvation (-3.4 ± 4.9 kcal/mol) (**Table S2**). The Buried Surface Area (BSA) value was 2139.2 ± 51.6 Å^2 (**Table S2**).

Discussion

The COVID-19 pandemic caused by SARS-CoV-2 remains a significant global health concern. Traditionally, antibodies have been considered essential components for diagnosis and treatment. However, due to the time and costs associated with antibody production, phage display technology has emerged as an alternative method for obtaining peptide-binding epitopes. Peptides offer a more straightforward and economical option compared to antibodies.[15-19] In this study, we identified phage clones displaying 12 amino-acid peptides that bound to the RBD of SARS-CoV-2 (RBD-SARS-CoV-2). The selected five phage clones demonstrated binding values > 0.5 OD_{450nm} after subtracting nonspecific binding. Displayed peptides of the selected five phage clones were further examined for binding activities. Short peptides often exhibit poor solubility and stability. As shown in **Table 1**, PepCalc analysis identified three good water-soluble peptides (RB 9, 10, and 56) and three poor water-soluble peptides (RB 5, 54, and UTP). To avoid solubility and stability issues, this study expressed peptides from the selected five phage clones as fused C-terminal peptides of bacterial Thioredoxin (Trx) to enhance solubility and heat stability (**Table 1**).[24,25] Predicted structure of the chimeric Trx-peptide (Trx-RB) generating by ColabFold[22] demonstrated that the Trx retained its structure while 40-amino-acid spacers and the peptides remained non-structured, suggesting a high flexibility of the C-terminal peptide (**Figure S2 b-f**). The fused peptides in this construct can interact with the RBD without hindrance from Trx. Additionally, chimeric Trx fused with an unrelated target peptide (Trx-UTP), similar to Trx-RB, was used as a negative control in all experiments. The results of all assays showed that Trx-UTP had low binding to both the RBD variants and the Omicron trimeric S. Thus, the results of the Trx-RB binding to the RBD were specifically attributed to the fused RB peptides.

As mentioned before, the SARS-CoV-2 virus exhibits a remarkable ability to adapt and undergo genetic changes, with multiple variants reported within one year.[4-6] Alignment of amino acid residues of SARS-CoV-2 with three other variants, Delta (B.1.617.2), Omicron (B.1.1.529), and XBB, revealed sequence similarities of 98.9%, 92.4%, and 88.9% with SARS-CoV-2, respectively (**Figure S3**). The mutated amino acid residues among the four SARS-CoV-2 variants were in the RBD regions, resulting in weak affinity of neutralizing antibodies to the viral particles,[26,27] particularly to XBB[28] (**Figure S3**). Interestingly, only 2 selected peptides, Trx-RB9 and Trx-RB10, had cross-bound the RBD of SARS-CoV-2 and variants, Delta, Omicron, and XBB. The Trx-RB9 binding the RBD of SARS-CoV-2 and the Omicron with an OD_{450nm} value higher than that of the Trx-RB10. However, to the RBD of the Delta and the XBB, both Trx-RB9 and Trx-RB10 had similar binding OD_{450nm} values. These results suggested that both Trx-RB9 and Trx-RB10 had different binding sites that were less affected by mutations (**Figure 5 a, b**). In addition, the results of no reduction in competition binding to the Omicron trimeric S also confirmed this observation. The structural differences between the trimeric S protein (aa27-1146), consisting of S1 and S2, and the monomeric RBD (aa328-525) may also influence the binding affinity of the chimeric peptides (**Figure S4**). The increased binding OD_{450nm} values of Trx-RB9 and Trx-RB10 to the Omicron trimeric S suggests the potential binding behavior of the chimeric peptides to the Omicron viral particle. The EC_{50} values of Trx-RB9 and Trx-RB10 for binding to the Omicron trimeric S were 111.9 and 360.2 nM, respectively, in contrast to 1.64 nM for the recombinant ACE2. Moreover, individually, either Trx-RB9 or Trx-RB10 could inhibit the binding of the recombinant ACE2 by < 10%. However, a mixture of 250 nM of both Trx-RB9 and Trx-RB10 inhibited 75% binding of the recombinant ACE2 to the Omicron trimeric S. The results suggest that Trx-RB9 and Trx-RB10 bind at different locations. The binding of Trx-RB9 and Trx-RB10 may partially interfere with the amino acids involved in the interaction between ACE2 and the RBD (**Figure 5a, b**; S5). When comparing the predicted binding sites of Trx-RB10 with the reported crystal structure of ACE2 binding to the RBD of the Omicron,[29] Trx-RB10 interacted with the RBD at the same reported residues: Ala484, Arg493, Ser496, and His505. However, the predicted binding site of Trx-RB9 did not overlap with that of hACE2. Moreover, when comparing the predicted binding site of ACE2 binding to the RBD of the Omicron trimeric S (**Figure S5**) with the reported crystal structure of ACE2 binding to the RBD of the Omicron,[29] only three residues, Arg493, Arg498, and Tyr501, are identical. The molecular docking also predicted additional binding site residues: Arg403, Val445, Ser446, Ala475, Asn477, Cys488, Pro499, and Thr500 (**Figure S5**). However, Pro499 and Thr500 of the predicted model are located adjacent to Arg498 and Tyr501 of the crystal structure.[29] Since both Arg498 and Tyr501 form a new interaction network in the hot spot-353 of the ACE2/Omicron RBD interface,[29] Pro499 and Thr500 of the predicted model may also be important for hACE2 interaction. This discrepancy might be due to the docking model, as this study used data from two crystal models, whereas the reported crystal structure was from recombinant hACE2 binding to the recombinant RBD region of the Omicron variant.[29] Taken together, it is possible that the binding site of Trx-RB10 overlaps with that of ACE2 in the ACE2/Omicron RBD interface. In addition to binding with both the RBD and the trimeric S, the binding activity of both chimeric peptides to the inactivated SARS-CoV-2 viral particle in Vero cell lysate also confirms that both chimeric peptides could interact with the S protein of the SARS-CoV-2 viral particle.

Molecular docking using the HADDOCK generated 36 predicted models in 4 distinct groups with different binding sites on the RBD of the Omicron trimeric S for both Trx-RB9 and Trx-RB10. The results suggest diversity in the predicted binding modes or interaction configurations. The RMSD of the predicted models is 25.3 ± 0.5 Å, indicating high instability of Trx-RB, which may result from the fused non-structured 40-amino-acid spacer and avitag-RB peptides (**Figure S2**). The high RMSD value agrees with the ColabFold-predicted structure, which shows structured Trx linked to non-structured 40-amino-acid spacer and avitag-RB peptides (**Figure S2**). The negative energy values of Van der Waals, Electrostatic, and Desolvation of the predicted models indicate favorable binding affinity between different components of the docked molecules. A high Buried Surface Area (BSA) value suggests a large interface area, indicating a stable protein-protein interaction. However, there were potential issues with the generated models, as noted in a high value of Restraints violation energy. In addition to molecular docking of Trx-RB binding to the RBD of the Omicron trimeric S, docking of hACE2 binding to the RBD of the Omicron trimeric S was also performed, along with a ChimeraX-generated model (**Table S2**, **Figure S5**). As previously mentioned, comparing the predicted binding sites of ACE2 binding to the RBD of the Omicron trimeric S with those of Trx-RB9 and Trx-RB10 suggests that only the predicted binding sites of Trx-RB10 may overlap with those of hACE2.

Phage display has been utilized to identify peptides that bind to the RBD of SARS-CoV-2 for either neutralization[30,31] or detection purposes.[32,33] However, owing to constant mutations in the RBD regions of the spike protein, it remains unclear whether previously reported peptides could cross-bind among different SARS-CoV-2 variants. Despite the presence of four different amino acids (484, 493, 496, and 505) in the RBD of SARS-CoV-2, Delta, and Omicron, both Trx-RB9 and Trx-RB10 demonstrated cross-binding with the RBD of the mutated variants, including the recent variant XBB.

Taken together, the chimeric Trx-RB9 and Trx-RB10 peptides exhibited binding with the RBD of multiple SARS-CoV-2 variants. Additionally, a combination of Trx-RB9 and Trx-RB10 peptides effectively inhibits the binding of recombinant human ACE2 to the RBD of the Omicron trimeric S. Further experiments are required to explore the therapeutic and detection potentials of Trx-RB9 and Trx-RB10, which are crucial for their practical applications in combating SARS-CoV-2.

Conflicts of interest

The authors declare no conflict of interest.

Acknowledgments

This work is supported by a grant (102849) from National Research Council of Thailand (the budget year 2564). P.U. was a Ph.D scholar of the Development and Promotion of Science and Technology Talents Project, Thailand. The authors would like to thank Prof. Emeritus. Dr. Pilaipan Puthavathana, Faculty of Medical Technology, Mahidol University, Thailand for kindly provide SARS-CoV-2 virus. Ms Kunjimas Ketsuwan, Center for Vaccine Development, Institute of Molecular Biosciences, Mahidol University, Thailand for preparation of the inactivated SARS-CoV-2.

Author Contributions

- PU. Investigation; writing – original draft.
- JP. Investigation; writing – editing; contributed new reagents/analytical tools.
- IM. Investigation; writing – editing; contributed new reagents/analytical tools.
- PM. Investigation; writing – editing; contributed new reagents/analytical tools.
- JK. Investigation; contributed new reagents/analytical tools.
- SP. Conceptualization; Supervision; investigation; writing – review and editing.

References

1. Chen N, Zhou M, Dong X, Qu J, Gong F, Han Y, et al. Epidemiological and clinical characteristics of 99 cases of 2019 novel coronavirus pneumonia in Wuhan, China: a descriptive study. Lancet. 2020;395: 507–13.
2. Yang X, Yu Y, Xu J, Shu H, Xia J, Liu H, et al. Clinical course and outcomes of critically ill patients with SARS-CoV-2 pneumonia in Wuhan, China: a single-centered, retrospective, observational study. Lancet Respir Med. 2020;8:475-81.
3. World Health Organization. WHO COVID-19 dashboard [Internet]. Geneva (CH): WHO; 2020. [updated 2023; cited 2023 Oct 20]. Available from: https://data.who.int/dashboards/covid19/cases?n=o
4. Mittal A, Manjunath K, Ranjan RK, Kaushik S, Kumar S, Verma V. COVID-19 pandemic: Insights into structure, function, and hACE2 receptor recognition by SARS-CoV-2. PLoS Pathog. 2020;16(8):e1008762.
5. Hardenbrook NJ, Zhang P. A structural view of the SARS-CoV-2 virus and its assembly. Curr Opin Virol. 2022;52:123-34.
6. Huang Y, Yang C, Xu XF, Liu S. Structural and functional properties of SARS-CoV-2 spike protein: potential antiviral drug development for COVID-19. Acta Pharmacol Sin. 2020;41:1141-9.
7. Fan Y, Li X, Zhang L, Wan S, Zhang L, Zhou F. SARS-CoV-2 Omicron variant: recent progress and future perspectives. Sig Transduct Target Ther. 2022;7(1):141-51.
8. Wang Q, Zhang Y, Wu L, Niu S, Song C, Zhang Z, et al. Structural and functional basis of SARS-CoV-2 entry by using human ACE2. Cell. 2020;181:894-904.
9. Yu S, Zheng X, Zhou B, Li J, Chen M, Deng R, et al. SARS-CoV-2 Spike engagement of ACE2 primes S2′ Site cleavage and fusion initiation. PNAS. 2022;119:e2111199119.
10. Chen Y, Zhao X, Zhou H, Zhu H, Jiang S, Wang P. Broadly neutralizing antibodies to SARS-CoV-2 and other human coronaviruses. Nat Rev Immunol. 2023;23:189–99.

11. Li H, Zhou B, Li B, Chen L, Ning X, Dong H. Isolation of a human SARS-CoV-2 neutralizing antibody from a synthetic phage library and its conversion to fluorescent biosensors. Sci Rep. 2022;12:15496.
12. Davies NG, Abbott S, Barnard RC, Jarvis CI, Kucharski AJ, Munday JD, et al. Estimated transmissibility and impact of SARS-CoV-2 lineage B.1.1.7 in England. Science. 2020;372:eabg3055.
13. Singh J, Rahman SA, Ehtesham NZ, Hira S, Hasnain SE. SARS-CoV-2 variants of concern are emerging in India. Nat Med. 2021;27:1131–3.
14. Costa CFS, Barbosa AJM, Dias AMGC, Roque ACA. Native, engineered and de Novo designed ligands targeting the SARS-CoV-2 spike protein. Biotechnol Adv. 2020;59:107986.
15. Souza PFN, Tilberg MFV, Mesquita FP, Amaral JL, Lima LB, Montenegro RC, et al. Neutralizing effect of synthetic peptides toward SARS-CoV-2. ACS Omega. 2020;7:16222-34.
16. Li T, Kan Q, Ge J, Wan Z, Yuan M, Huang Y, et al. A novel linear and broadly neutralizing peptide in the SARS-CoV-2 S2 protein for universal vaccine development. Cell Mol Immunol. 2021;18:2563–5.
17. Wolfe M, Webb S, Chushak Y, Krabacher R, Liu Y, Swami N, et al. A high-throughput pipeline for design and selection of peptides targeting the SARS-Cov-2 Spike protein. Sci Rep. 2021;11:21768.
18. Huang X, Pearce R, Zhang Y. Computational design of peptides to block binding of the SARS-CoV-2 spike protein to human ACE2. Aging. 2020;12(12):11263-76.
19. Thakkar R, Agarwal DK, Ranaweera CB, Ishiguro S, Conda-Sheridan M, Gaudreault NN, et al. De novo design of a stapled peptide targeting SARS-CoV-2 spike protein receptor-binding domain. RSC Med Chem. 2023;14(9):1722-33.
20. Wu CH, Liu IJ, Lu RM, Wu HC. Advancement and applications of peptide phage display technology in biomedical science. J Biomed Sci. 2016;23:8.
21. Anand T, Virmani N, Bera BC, Vaid RK, Vashisth M, Bardajatya P, et al. Phage display technique as a tool for diagnosis and antibody selection for coronaviruses. Curr Microbiol. 2021;74:1124-34.
22. Mirdita M, Schütze K, Moriwaki Y, Heo L, Ovchinnikov S, Steinegger M. ColabFold: making protein folding accessible to all. Nat Methods. 2022;19:679–82.
23. Zundert GCPV, Rodrigues JPGLM, Trellet M, Schmitz C, Kastritis PL, Karaca E, et al. The HADDOCK22 web server: User-friendly integrative modeling of biomolecular complexes. J Mol Biol. 2016;428:720–5.
24. Al Musaimi O, Lombardi L, Williams DR, Albericio F. Strategies for Improving Peptide Stability and Delivery. Pharmaceuticals (Basel). 2022;15(10):1283.
25. Schenkel M, Treff A, Deber CM, Krainer G, Schlierf M. Heat treatment of thioredoxin fusions increases the purity of α-helical transmembrane protein constructs. Protein Sci. 2021;30:1974-82.
26. Patrick C, Upadhyay V, Lucas A, Mallela KMG. Biophysical Fitness Landscape of the SARS-CoV-2 Delta Variant Receptor Binding Domain. J Mol Biol. 2022;13:167622.
27. Cao Y, Wang J, Jian F, Xiao T, Song W, Yishimayi A, et al. Omicron escapes the majority of existing SARS-CoV-2 neutralizing antibodies. Nature. 2022;602:657-63.
28. He Q, Wu L, Xu Z, Wang X, Xie Y, Chai Y, et al. An updated atlas of antibody evasion by SARS-CoV-2 Omicron sub-variants including BQ.1.1 and XBB. Cell Rep Med. 2023;4:100991.
29. Geng Q, Shi K, Ye G, Zhang W, Aihara H, Li F. Structural Basis for Human Receptor Recognition by SARS-CoV-2 Omicron Variant BA.1. J Virol. 2022;96(8):e0024922.
30. Passariello M, Gentile C, Ferrucci V, Sasso E, Vetrei C, Fusco G, et al. Novel human neutralizing mAbs specific for Spike-RBD of SARS-CoV-2. Sci Rep. 2021;11:11046.
31. Yao H, Wang H, Zhang Z, Liu Y, Zhang Z, Zhang Y, et al. A potent and broad-spectrum neutralizing nanobody for SARS-CoV-2 viruses, including all major Omicron strains. MedComm. 2020;4(6):3397.
32. Yang F, Liu L, Neuenschwander PF, Idell S, Vankayalapati R, Jain KG, et al. Phage display-derived peptide for the specific binding of SARS-CoV-2. ACS Omega. 2022;7:3203-11.
33. Pang S, Yu H, Zhang Y, Jiao Y, Zheng Z, Wang M, et al. Bioscreening specific peptide-expressing phage and its application in sensitive dual-mode immunoassay of SARS-CoV-2 spike antigen. Talanta. 2023;266: 125093.

Supplementary Methods

Phage display selection against the RBD of SARS-CoV-2

Biopanning

Briefly, the beads were incubated with 10^{11} pfu/mL of PhD-12 Phage display library (NEB, USA) at room temperature (RT) for 1 hour with gentle agitation. After a 10-time washing with TBS-0.1% Tween-20 (T), the beads were incubated in an elution solution (0.2 M glycine, pH 2.2) for 20 minutes. Subsequently, the supernatant was neutralized to pH 7.4 with 1 M Tris-HCl, pH 9.1 solution in a new tube. The supernatant containing phages were incubated with *E. coli* ER2738 (NEB, USA) culture containing 50 μg/mL tetracycline at 37°C for 4.5 hours. The culture was centrifuged at 9,300 ×g for 30 minutes, and the supernatant was used for the next round. The second and third rounds of biopanning were performed the same as above, except for washing the beads with TBS-0.5%T.

Phage ELISA

The eluted phages binding the RBD of SARS-CoV-2 was determined. An amount of 188.68 nM of the RBD in PBS-1% BSA was incubated in each well of a 96-well Maxisorp plate (Nunc, USA) at 4°C overnight. After washing with PBS-0.05%T, PBS-0.05%T-1%BSA was added and incubated at RT for 1 hour. After washing, a mixture containing 50 μL of 10^9 pfu/mL amplified phages and 50 μL of PBS-0.05%T was incubated per well at RT for 2 hours. After washing, a 1:250 diluted HRP-labeled mouse IgG anti-M13 phage (Abcam, UK) was incubated at RT for 1 hour. After washing, TMB (3,3′,5,5′-Tetramethylbenzidine) was added, and the reaction was stopped by adding 2 M sulfuric acid before measuring absorption at OD_{450nm}.

Expression and purification of chimeric peptides

The phage-derived 12-amino-acid peptides were expressed as chimeric fused-protein. An avidin tag was added at the N-terminus and 6xHis tag was added at the C-terminus of the peptides. The cDNA encoding the peptides was synthesized and inserted into a cloning site at a C-terminus of bacterial Thioredoxin (Trx) of plasmid pET32b (GenScript, USA). The plasmid was transformed into *E. coli* T7 express lysY (NEB, USA) and grown on LB plates containing 100 μg/mL ampicillin and 20 μg/mL chloramphenicol. Chimeric Trx-peptides were expressed under 0.2 mM IPTG induction at 25°C for 6 hours. Bacterial pellets containing Trx-peptides were sonicated in PBS-lysozyme and centrifuged at 16,000 ×g at 4°C for 30 minutes. The supernatant containing Trx-peptides was incubated with Ni^{2+} magnetic beads in buffer-A (50 mM NaH_2PO_4, 0.3 M NaCl, and 20 mM imidazole) at RT for 30 minutes with gentle shaking. After washing with buffer-A,

Trx-peptides were eluted with buffer-B (50 mM NaH_2PO_4, 0.3 M NaCl, and 250 mM imidazole) before being stored at -20°C. In addition to Trx-RB, a chimeric Trx fused with an unrelated target peptide (Trx-UTP), a construct similar to Trx-RB, was expressed and prepared as described above and used in all experiments.

Direct binding of Chimeric Trx-peptides

The avidin tags of Trx-peptides (Trx-RB) and Trx-unrelated peptide (Trx-UTP) were biotinylated using a biotinylation kit (Abcam, UK). Binding of biotinylated Trx-RB and Trx-UTP to recombinant RBD (aa328-525) of the S1 of variants, including SAR-CoV-2, Delta, Omicron, and XBB (Sino biological, China), was performed as follows. An amount of 188.68 nM of the RBD in PBS were incubated per well of a 96-well maxisorp plate at 4°C overnight. After washing with PBS-0.05%T, PBS-0.05%T-3% (W/V) non-fat dried milk (NFDM) was added and incubated at RT for 1 hour. After washing with PBS-0.05%T, 250 nM of biotinylated Trx-RB was added and incubated at RT for 1.5 hours with gentle shaking. After washing, 1:4000 diluted HRP-conjugated streptavidin (HRP-Strepavidin, Abcam, UK) was added and incubated at RT for 1 hour. After washing, TMB substrate was added, and the reaction was stopped by adding 2 M sulfuric acid before measuring absorption at OD_{450nm}.

EC_{50} determination assay using the SARS-CoV-2 (B.1.1.529) trimeric S

To determine the half-maximal effective concentration (EC50), Trx-peptides (Trx-RB) binding recombinant trimeric S (S1 + S2) of SARS-CoV-2 (B.1.1.529, Omicron) (Omicron trimeric S) (Sino Biological, China) was performed as follows. 7.14 nM of Omicron trimeric S in PBS was incubated per well of a 96-well maxisorp plate at 4°C overnight. After washing with PBS-0.05%T, PBS-0.05%T-3%NFDM was added and incubated at RT for 1 hour. After washing, a serial diluted 0.1 to 600 nM biotinylated Trx-RB9 and Trx-RB10 were added. Moreover, a serial diluted 0.01 to 100 nM recombinant human ACE2 with a human FC tag (ACE2-FC) (Sino Biological, China) was also added as the control. Then, 1:4000 diluted HRP-Streptavidin was added to detect the bound Trx-RB9 and Trx-RB10, while HRP-conjugated anti-human IgG antibody (Abcam, UK) was added to detect bound ACE2, and incubated at RT for 1 hour. After washing, TMB substrate was added, and the reaction was stopped by adding 2 M sulfuric acid before measuring absorption at OD_{450nm}.

Analysis of binding sites of chimeric Trx-RB on the RBD of the SARS-CoV-2 (B.1.1.529) trimeric S

The binding sites of Trx-RB9 and Trx-RB10 on the RBD of the Omicron trimeric S was determined in 2 tests as follows.

In competitive ELISA, 7.14 nM of Omicron trimeric S in PBS, were added per well of a 96-well maxisorp plate and incubated at 4°C overnight. After washing with PBS-0.05%T, PBS-0.05%T-3%NFDM was added and incubated at RT for 1 hour. After washing, 100 nM biotinylated-Trx-RB10 was added. Then, various dilutions of Trx-RB9 (0, 62.5, 125, 250, 500 nM) were added and incubated at RT for 2 hours. After washing, 1:4000 diluted HRP-Streptavidin was added and incubated at RT for 1 hour. After washing, TMB substrate was added, and the reaction was stopped by adding 2 M sulfuric acid before measuring absorption at OD_{450nm}.

In Western blot, 59.52 nM of Omicron trimeric S was loaded per lane of a 10% SDS-PAGE gel, and resolved under a constant current before being transferred onto a nitrocellulose membrane. The membrane was cut as strips and incubated in PBS-0.05%T-3%NFDM at RT for 1 hour. Then, each membrane strip was incabated with 5 nM ACE2-Fc or a mixture of 5 nM ACE2-Fc and 500 nM Trx-RB9 and/or Trx-RB10 at RT for 2 hours. After washing with PBS-0.05%T, each membrane strip was incabated with 1:4000 diluted HRP-conjugated anti-human Fc-IgG antibody (Abcam, UK) at RT for 1 hour. After washing, each membrane strip was incabated with chemiluminescent HRP substrate, and emitted signals were captured on X-ray film. The intensity of the bands was analyzed using Image J software before values were converted to the percentage of ACE2 binding.

Direct ELISA of the chimeric Trx-RB binding the inactivated SARS-CoV-2

SARS-CoV-2 (2019-nCoV; MUMT64019039) propagation and inactivation were prepared by the Center for Vaccine Development, Institute of Molecular Biosciences, Mahidol University, Thailand, as follows. African kidney Vero cells (ATCC No. CCL-81) were cultured in Dulbecco's Modified Eagle's Medium (DMEM) (Gibco, USA) containing 10% fetal bovine serum (FBS) (Hyclone, USA) at 37°C with 5% CO_2. The virus was propagated in the Vero cells cultured in DMEM-2%FBS. The virus was harvested by centrifugation, and the titer was determined by plaque assay. SARS-CoV-2 supernatant containing 1×10^8 pfu/mL was inactivated by Lysis Buffer (4% v/v SDS, 250 mM Tris-HCl pH 6.8, 0.9 mM Bromophenol blue, 0.5 mM DTT, 30% v/v Glycerol) and boiled for 5 minutes.

For ELISA, a diluted 10^2-10^7 pfu/mL of inactivated SARS-CoV-2 in PBS was incubated per well of a 96-well maxisorp plate at 4°C overnight. After washing with PBS-0.05%T, PBS-0.05%T-3%NFDM was added and incubated at RT for 1 hour. After washing, 600 nM of biotinylated-Trx-RB9, or Trx-RB10, or Trx-UTP, was added and incubated at RT for 1.5 hours with gentle shaking. After washing, 1:4000 diluted HRP-Streptavidin was added and incubated at RT for 1 hour. After washing, TMB substrate was added, and the reaction was stopped by adding 2 M sulfuric acid before measuring absorption at OD_{450nm}.

Supplemental Table S1. HADDOCK analysis score of chimeric Trx-RB9 and Trx-RB10 interacting the RBD of the Omicron monomeric spike (PDB:7WPB)

HADDOCK score	-97.6 ± 19.4
Cluster size	4
RMSD from the overall lowest-energy structure	25.3 ± 0.5 Å
Van der Waals energy	-76.4 ± 13.9 kcal/mol
Electrostatic energy	-297.0 ± 38.5 kcal/mol
Desolvation energy	-3.3 ± 2.7 kcal/mol
Restraints violation energy	414.1 ± 111.65 kcal/mol
Buried Surface Area	2420.8 ± 192.4 Å^2
Z-Score	-0.8

Supplemental Table S2. HADDOCK analysis score of hACE2 (PDB: 6JWH) interacting the RBD of the Omicron monomeric spike (PDB:7WPB)

HADDOCK score	-97.0 ± 1.7
Cluster size	13
RMSD from the overall lowest-energy structure	3.3 ± 0.4 Å
Van der Waals energy	-53.5 ± 6.6 kcal/mol
Electrostatic energy	-383.0 ± 13.9 kcal/mol
Desolvation energy	-3.4 ± 4.9 kcal/mol
Restraints violation energy	365.2 ± 58.8 kcal/mol
Buried Surface Area	2139.2 ± 51.6 Å^2
Z-Score	-2.0

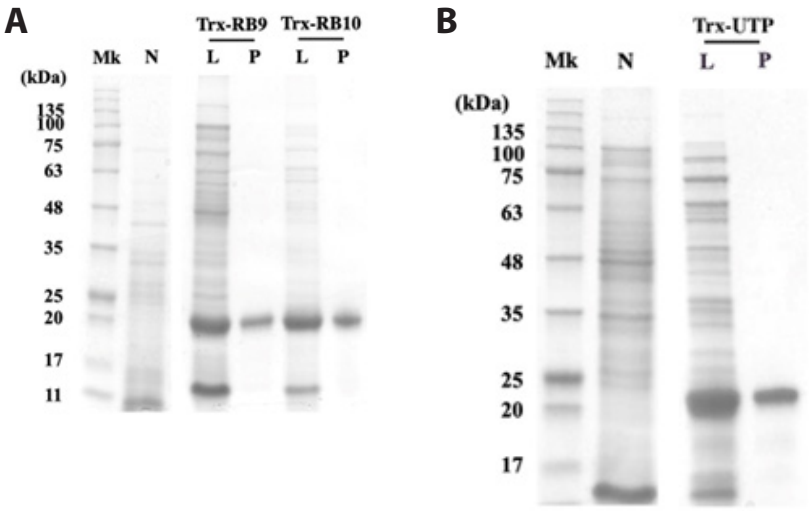

Supplemental Figure S1. Trx-RBs expression and purification. (a-b) SDS-PAGE analysis was performed to examine the expression and purification of (a) Trx-RB9, Trx-RB10, and (b) Trx-UTP. Samples with 0.2 OD600nm value and 500 ng of purified Trx-RBs were loaded. Note: Mk = protein marker, N = non induced sample, L = induced cell lysates, P = purified samples.

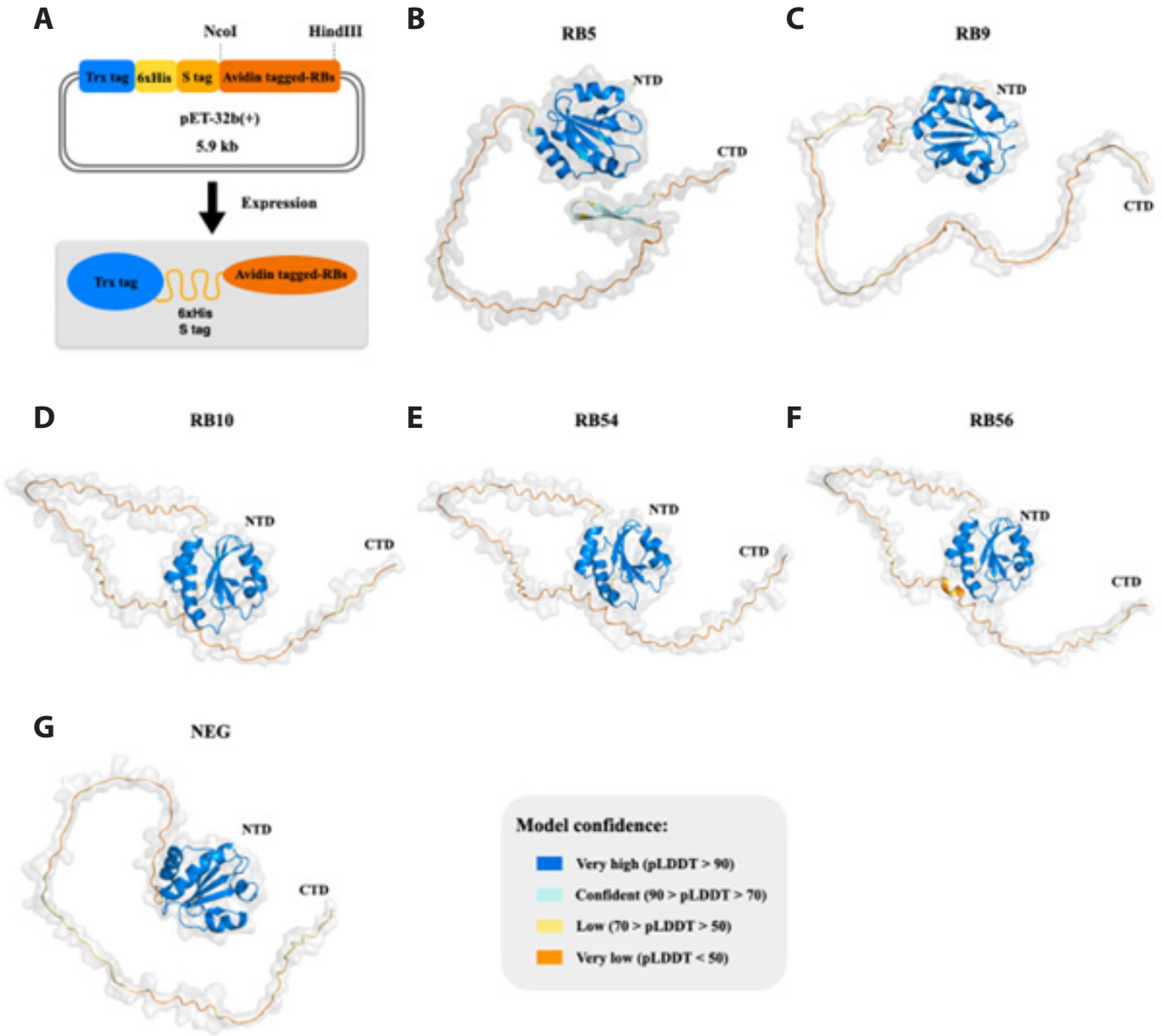

Supplemental Figure S2. A) Illustration of Trx-peptide construct; B) Predicted 3D-structure of chimeric peptides generated by the ColabFold

```
2019-nCoV   333  TNLCPFGEVF NATRFASVYA WNRKRISNCV ADYSVLYNSA SFSTFKCYGV SPTKLNDLCF  392
B.1.617.2   333  TNLCPFGEVF NATRFASVYA WNRKRISNCV ADYSVLYNSA SFSTFKCYGV SPTKLNDLCF  392
B.1.1.529   333  TNLCPFDEVF NATRFASVYA WNRKRISNCV ADYSVLYNLA PFFTFKCYGV SPTKLNDLCF  392
XBB         333  TNLCPFHEVF NATTFASVYA WNRKRISNCV ADYSVIYNFA PFFAFKCYGV SPTKLNDLCF  392

2019-nCoV   393  TNVYADSFVI RGDEVRQIAP GQTGKIADYN YKLPDDFTGC VIAWNSNNLD SKVGGNYNYL  452
B.1.617.2   393  TNVYADSFVI RGDEVRQIAP GQTGKIADYN YKLPDDFTGC VIAWNSNNLD SKVGGNYNYR  452
B.1.1.529   393  TNVYADSFVI RGDEVRQIAP GQTGNIADYN YKLPDDFTGC VIAWNSNKLD SKVSGNYNYL  452
XBB         393  TNVYADSFVI RGNEVSQIAP GQTGNIADYN YKLPDDFTGC VIAWNSNKLD SKPSGNYNYL  452

2019-nCoV   453  YRLFRKSNLK PFERDISTEI YQAGSTPCNG VEGFNCYFPL QSYGFQPTNG VGYQPYRVVV  512
B.1.617.2   453  YRLFRKSNLK PFERDISTEI YQAGSKPCNG VEGFNCYFPL QSYGFQPTNG VGYQPYRVVV  512
B.1.1.529   453  YRLFRKSNLK PFERDISTEI YQAGNKPCNG VAGFNCYFPL RSYSFRPTYG VGHQPYRVVV  512
XBB         453  YRLFRKSKLK PFERDISTEI YQAGNKPCNG VAGPNCYSPL QSYGFRPTYG VGHQPYRVVV  512

2019-nCoV   513  LSFELLHAPA TVCGPKKST 531
B.1.617.2   513  LSFELLHAPA TVCGPKKST 531
B.1.1.529   513  LSFELLHAPA TVCGPKKST 531
XBB         513  LSFELLHAPA TVCGPKKST 531
```

Supplemental Figure S3. Alignment of Amino Acid Sequences from the RBD of Four SARS-CoV-2 Variants. Amino acid sequences from the RBD of SARS-CoV-2 compared to those of Delta (B.1.617.2), Omicron (B.1.1.529), and XBB. Different residues are highlighted

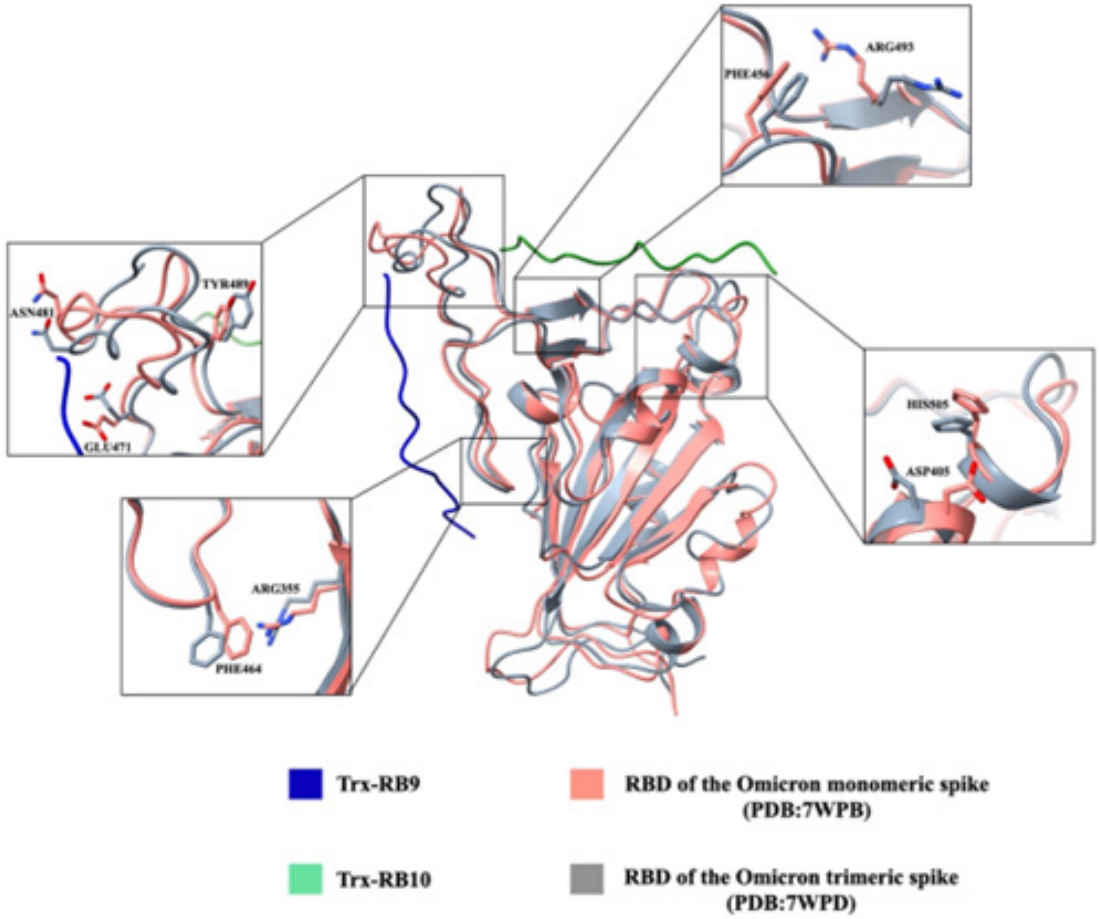

Supplemental Figure S4. Structural Comparison of Two Recombinant RBDs from the Omicron Spike. Structural comparison of the RBD of the Omicron monomeric spike (PDB:7WPB) (pink) and the RBD of the Omicron trimeric spike (PDB:7WPD) (gray) using ChimeraX. Peptides RB9 (blue) and RB10 (green) interact with both structures. The inset shows amino acid residues with differences in terms of angle and location.

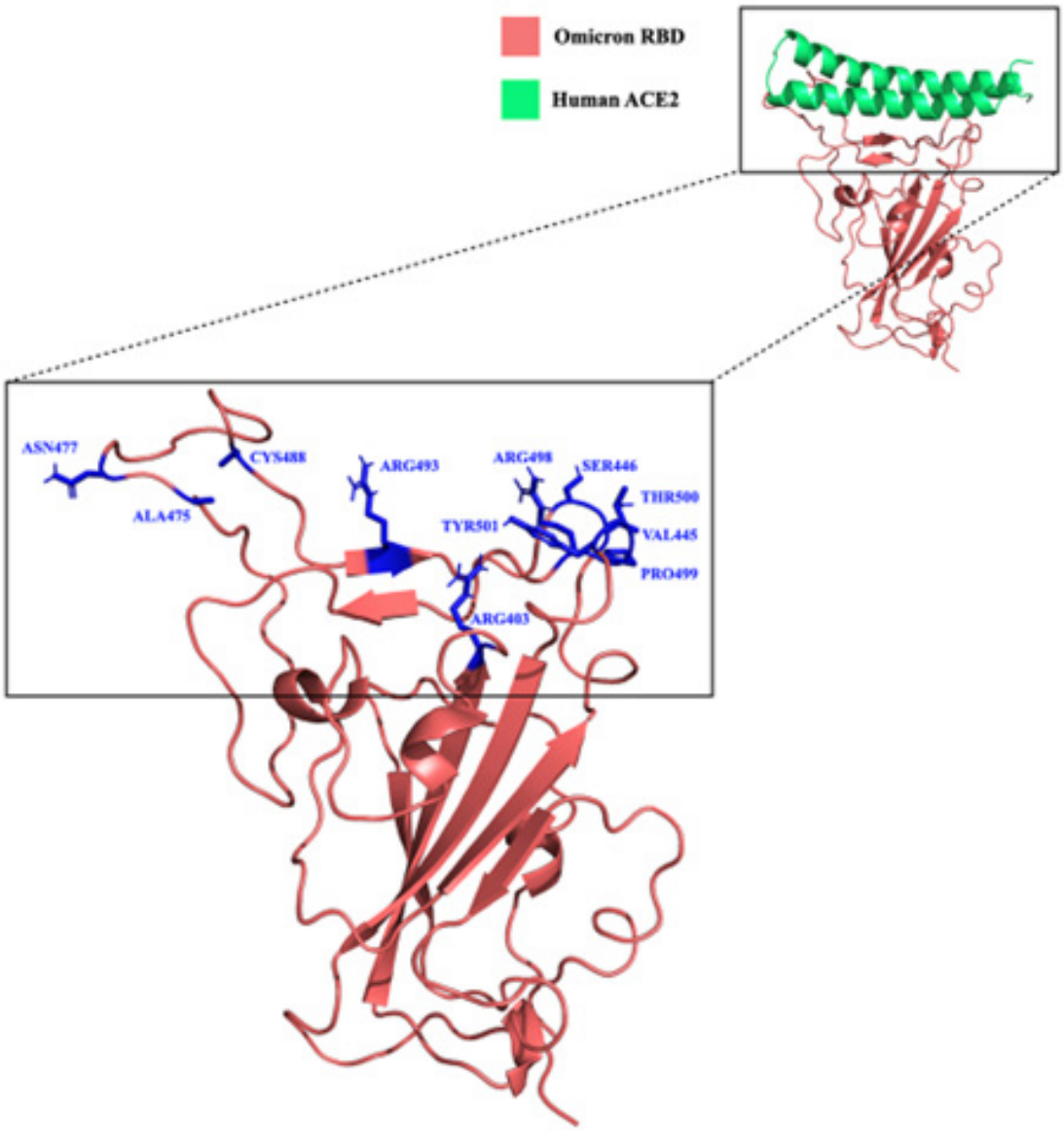

Supplemental Figure S5. Molecular docking of hACE2 binding to the RBD of the Omicron trimeric spike (PDB:7WPB). The alpha1-2 regions of hACE2 (PDB: 6JWH) interacting to amino acids of RBD of the Omicron trimeric spike (PDB:7WPD) from ChimeraX-generated structure of the hACE2 binding to the RBD is showed. The inset shows interacted amino acid residues of RBD.